Structure of the Atmosphere of Jupiter: Galileo Probe Measurements

Alvin Seiff,* Donn B. Kirk, Tony C. D. Knight, John D. Mihalov, Robert C. Blanchard, Richard E. Young, Gerald Schubert, Ulf von Zahn, Gerald Lehmacher, Frank S. Milos, Jerry Wang

Temperatures and pressures measured by the Galileo probe during parachute descent into Jupiter's atmosphere essentially followed the dry adiabat between 0.41 and 24 bars, consistent with the absence of a deep water cloud and with the low water content found by the mass spectrometer. From 5 to 15 bars, lapse rates were slightly stable relative to the adiabat calculated for the observed H_2/He ratio, which suggests that upward heat transport in that range is not attributable to simple radial convection. In the upper atmosphere, temperatures of >1000 kelvin at the 0.01-microbar level confirmed the hot exosphere that had been inferred from Voyager occultations. The thermal gradient increased sharply to 5 kelvin per kilometer at a reconstructed altitude of 350 kilometers, as was recently predicted. Densities at 1000 kilometers were 100 times those in the preencounter engineering model.

The Galileo probe, using instruments and techniques previously described (*1*), measured state properties of Jupiter's atmosphere from nanobar pressure levels to a final pressure of ~24 bars. The depth reached in the probe's parachute descent, calculated from measured temperatures and pressures assuming hydrostatic equilibrium, was ~160 km or 0.22% of the radius of Jupiter. Velocities during descent decreased from ~400 m s^{-1} at parachute deployment to 156 m s^{-1} in the first 100 s, to ~48 m s^{-1} at the 3-bar level, and to ~30 m s^{-1} at loss of signal.

Temperatures measured in parachute descent had an accuracy of ~1 K and a dispersion on the order of the digital resolution (0.12 K) (*2*) (Fig. 1). Comparison with the Orton model (*3*) indicates that the atmosphere is close to a dry adiabat over this pressure range. Water condensation, expected above the 5-bar level if the oxygen mole fraction is solar [0.0017 (*4*)] and above the 4-bar level for the low water abundance detected by the neutral mass spectrometer [~0.2 of the solar abundance value (*5*)], has major effects on the temperature variation (*6*). Temperatures following the dry adiabat at these levels confirm the low water abundance and are consistent with the absence of a detectable water cloud (*7*). Deviations from the adiabat between 1 and 3 bars, which were initially interpreted as a stable layer in the tenuous cloud above 1.6 bars (*7*) and an unstable layer below the cloud, now are believed to reflect departures from preflight pressure sensor calibrations resulting from unanticipated variations in the probe's internal temperature (*8*).

The data, as corrected for temperature effects (*9*), start to diverge from the adiabat at pressures of >16 bars. The sensor continued to read until the probe signal was lost at a final pressure of 24 ± 1 bars. The final sensor temperature, 388 K, was only 37 K cooler than the atmospheric temperature at the end of descent.

The temperature lapse rates between the 5-bar and 16-bar levels, −1.8 ± 0.1 K km^{-1} (Fig. 2), were slightly stable against overturn relative to adiabatic lapse rates of −1.95 K km^{-1} for an atmosphere of the measured composition (*10*). This potentially important observation implies that heat flux within this layer is not by simple convection. Guillot *et al.* (*11*) found that, for Jupiter, radiative transport could predominate over convection in the absence of condensed water in the layer with temperatures of 200 to 500 K. Although the slightly subadiabatic temperature gradients could indicate that heat transport is radiative, stable lapse rates can occur in convective regions driven by convection at greater depths. The interpretation of the small degree of subadiabaticity requires additional study.

Transverse accelerations of the probe, measured in descent (Fig. 3), were transmitted in compact form as maximum, minimum, and average values of the resultant of the two orthogonal lateral axis accelerations over 16-s intervals. At pressures below 2.2 bars and above 7 bars, the accelerations were remarkably constant, with maxima ($a_{N_{max}}$, where a_N is acceleration normal to the probe axis of symmetry) of ~0.9 m s^{-2}. Such a record would be produced by a slightly elliptical swinging motion of the probe beneath the parachute (*12*) of peak amplitude $\alpha = \sin^{-1}(a_{N_{max}}/g_J) = 2.2°$, where g_J is Jupiter's gravitational acceleration. A simple pendulum with a length equal to that of the parachute cords (13.9 m) would swing in Jupiter's gravity field with a period of ~4.9 s. A 5-s period was seen in the amplitude of the probe radio signal (*13*). The sudden jumps in amplitude at 2.2 and 3.3 bars (Fig. 3), with subsequent slow decay back to the 2.2° swinging amplitude at 7 bars, could have been a result of the exposure of the sensors to the probe's cold internal environment (sensors reached 240 K, 13 K below their designed operating range), or they could have been stimulated by horizontal gusts. The jumps occur close to the level where the measured horizontal wind changes from an increasing profile to constant magnitude (*14*).

Upper atmospheric data recording be-

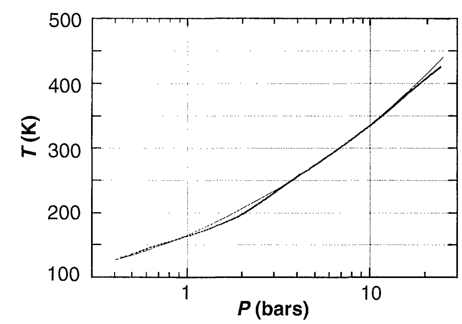

Fig. 1. Temperatures measured in descent as a function of pressure. The thick line is formed by the data points; the fine line is the Orton model (*3*).

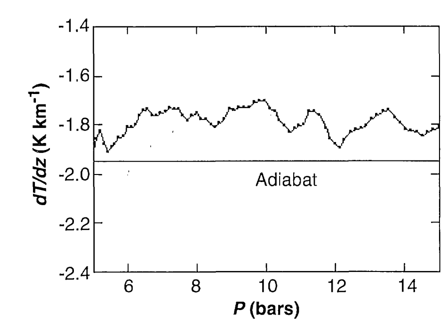

Fig. 2. Temperature lapse rates with altitude for altitudes below the 5-bar level. The adiabat is for the measured H_2/He ratio (*10*), for which the adiabat differs by −0.025 K km^{-1} from that in the Orton model.

A. Seiff, Department of Meteorology, San Jose State University, San Jose, CA 95192, USA.
D. B. Kirk, 37465 Riverside Drive, Pleasant Hill, OR 97455, USA.
T. C. D. Knight, 2370 South Brentwood Street, Lakewood, CO 80227, USA.
J. D. Mihalov, R. E. Young, F. S. Milos, J. Wang, NASA Ames Research Center, Moffett Field, CA 94035, USA.
R. C. Blanchard, NASA Langley Research Center, Hampton, VA 23681, USA.
G. Schubert, Department of Earth and Space Science, University of California, Los Angeles, CA 90024, USA.
U. von Zahn, Institut für Atmospharenphysik, Universität Rostock, D(0)-2565 Kühlungsborn, Germany.
G. Lehmacher, NASA Goddard Space Flight Center, Greenbelt, MD 20771, USA.

*To whom correspondence should be addressed. E-mail: al_seiff@qmgate.arc.nasa.gov

gan at a deceleration of 40 μg when probe velocity was 47.23 km s^{-1} relative to the atmosphere (*15*). Decelerations with an initial resolution of 3 μg and an altitude resolution of 1.75 km were recorded through seven decades of amplitude to a peak of 228*g*, afterwards diminishing toward $1g_J$. From these data and the initial conditions of velocity, path angle, and heading angle at entry (*16*), the entry trajectory was reconstructed to define velocity, flight path angle, and altitude from the experiment threshold to the time of parachute deployment. The final state of this trajectory was compared with initial conditions in descent, and small adjustments in initial conditions at entry were made to match conditions at the mode change. The reconstructed threshold altitude was 1019 km.

The upper atmospheric density profile $\rho(z)$ with respect to altitude z (Fig. 4) was calculated from the reconstructed velocities V, measured decelerations a, and knowledge of the drag coefficient $C_D(t)$, vehicle mass $m(t)$, and frontal area $A(t)$ (with respect to time t): $\rho = 2ma/(C_D A V^2)$. Drag coefficients accurate within ~1% were established by ballistic range tests (*17*) and computational fluid dynamics solutions (*18*). The density data essentially coincide with the Orton model below 290 km (*3*) but depart from it at higher altitudes; at 1000 km, densities were 100 times the model density. Pressures obtained under the assumption of hydrostatic equilibrium extend to a threshold pressure at 0.01 μbar.

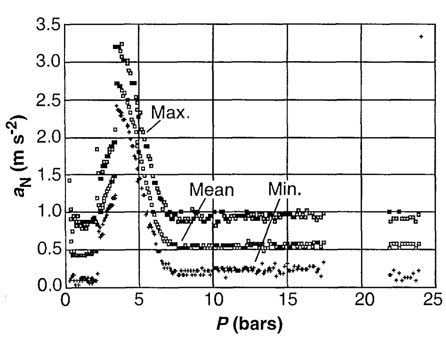

Fig. 3. Resultant accelerations perpendicular to the probe axis of symmetry. These are the highest, lowest, and average accelerations (max., min., mean) recorded in 16-s sampling intervals.

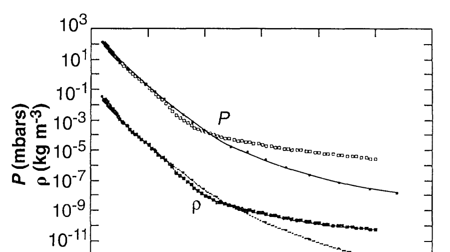

Fig. 4. Densities and pressures from probe deceleration data and the reconstructed trajectory. The lines are the Orton model (*3*).

Temperatures calculated from the equation of state applied to these profiles reach a maximum of 1350 K (Fig. 5) and suggest the presence of a superimposed wave structure. A constant mean molecular mass of 2.215 has been used to define the gas constant (*19*). The initial pressure chosen at 1000 km (Fig. 4) is a reasonable extension of the data below 800 km. Any subsequent refinements will not alter the basic observation: Jupiter's exosphere is hot.

The Voyager extreme ultraviolet solar occultation experiment (*20*) measured a Jovian exospheric temperature of 1450 ± 275 K at an unspecified altitude. Subsequent stellar occultations and improved analysis of the solar occultation, reviewed in (*21*), have yielded lower temperatures on which the models of the upper atmosphere in Fig. 5 were based (*3*). A more recent spectroscopic temperature, 540 ± 40 K at the 300-μbar level (*22*), indicates that the temperature rises rapidly above the 300-km level. The significance of this measurement was noted by Yelle *et al.* (*21*), whose preferred model (Fig. 5), with $(dT/dz)_{max}$ = 5 K km^{-1} at 375 km, matches the experimental slope well.

In view of Jupiter's great distance from the sun, such high exosphere temperatures require explanation. Such explanations have centered on two ideas: heating by gravity waves propagating up from the lower atmosphere (*20, 21*), and heating by soft electron collisions on H_2 molecules (*23*). Yelle *et al.* suggested that the sudden temperature rise above 300 km is associated with viscous damping of gravity waves propagating upward from the lower atmosphere and with the disappearance of methane, which provides radiative cooling.

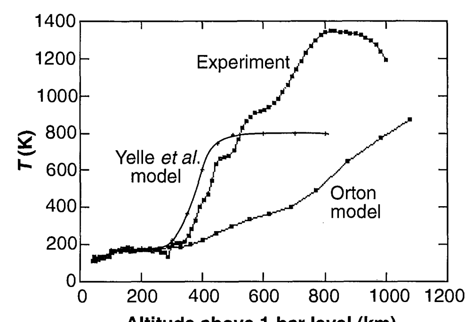

Fig. 5. Temperatures derived from pressures and densities in Fig. 4 and the equation of state. The major departure of the Orton model from the data at higher altitudes apparently results from a nearly linear interpolation between widely spaced temperature observations. The preferred model of Yelle *et al.* (*21*) is based on recent spectroscopic data that require rapid warming above 300 km.

REFERENCES AND NOTES

1. A. Seiff and T. C. D. Knight, *Space Sci. Rev.* **60**, 203 (1992).
2. The sensor was designed to avoid problems resulting from lightning strikes, electrical discharge, and shorting by condensibles.
3. G. S. Orton, *Jet Propulsion Laboratory Report 1625-125, NASA* (1981). Below 1 bar, the model is an adiabat for an atmosphere with mole fractions of 0.888 H_2, 0.112 He, 0.0017 CH_4, and 0.00022 NH_3.
4. H. B. Niemann *et al., Space Sci. Rev.* **60**, 111 (1992).
5. H. B. Niemann *et al., Science* **272**, 847 (1996).
6. A. D. Del Genio and K. B. McGrattan, *Icarus* **84**, 29 (1990).
7. B. Ragent, D. S. Colburn, P. Avrin, K. A. Rages, *Science* **272**, 855 (1996).
8. During parachute descent, probe internal temperatures varied from 223 to 388 K, exceeding the limits of 258 to 323 K for which the pressure sensors had been designed and calibrated. The correspondingly high rates of change of sensor temperature with time, up to 7.3 K min^{-1}, are an additional source of uncertainty because the sensors could not attain thermal equilibrium. Tests in progress of the engineering and flight spare sensors at temperatures and temperature rates similar to those in flight will indicate the effects of this operating environment on sensor offsets for use in correcting flight data.
9. For pressures between 5 and 17 bars, pressure sensor offsets were selected with guidance from sensors in the helium abundance detector (HAD). The HAD sensors, mounted in a block of nearly solid beryllium, experienced a smaller temperature range (254 to 301 K) than did the atmospheric structure instrument (ASI) sensors.
10. U. von Zahn and D. M. Hunten, *Science* **272**, 850 (1996).
11. T. Guillot, D. Gautier, G. Chabrier, B. Mosser, *Icarus* **112**, 337 (1994).
12. R. Preston, personal communication.
13. R. Woo, personal communication.
14. D. H. Atkinson, J. B. Pollack, A. Seiff, *Science* **272**, 842 (1996).
15. The upper atmospheric data period, 240 s, was dictated by probe memory capacity and ended at the start of parachute descent. Thus, the unplanned 53-s delay in the start of descent [R. E. Young, M. A. Smith, C. K. Sobeck, *Science* **272**, 837 (1996)] also delayed the start of entry data acquisition. With on-time deployment, the threshold would have been at the 3-μg level.
16. J. Neff, personal communication.
17. P. F. Intrieri, C. E. DeRose, D. B. Kirk, *Acta Astronaut.* **4**, 789 (1977); P. F. Intrieri and D. B. Kirk, *J. Spacecr. Rockets* **24**, 127 (1987).
18. B. L. Haas and F. S. Milos, *J. Spacecr. Rockets* **32**, 398 (1995); E. Venkatapathy, personal communication. Further computational fluid dynamics solutions have been made for the continuum flow regime and for the ablated heat shield shape.
19. As an initial assumption, the mean molecular mass used was a lower atmospheric value, 2.215. The upper atmosphere is believed to be dominated by molecular hydrogen [S. K. Atreya, T. M. Donahue, M. C. Festou, *Astrophys. J.* **247**, L43 (1981)]. Temperatures at the higher altitudes in Fig. 5 may thus be up to 10% too high.
20. S. K. Atreya, T. M. Donahue, B. R. Sandel, A. L. Broadfoot, G. R. Smith, *Geophys. Res. Lett.* **6**, 795 (1979).
21. R. V. Yelle *et al., J. Geophys. Res.* **101**, 2149 (1996).
22. W. Liu and A. Dalgarno, *Astrophys. J.*, in press.
23. D. M. Hunten and A. J. Dessler, *Planet. Space Sci.* **25**, 817 (1977).

24. We thank J. Lepetich and L. Yee, who served as ASI managers, for their contributions to this experiment. We also thank E. Tischler, C. Sobeck, and numerous other Probe Project Office personnel and those who contributed to the instrument design and development at Martin Marietta Aerospace and at Bell Aerospace.

4 March 1996; accepted 17 April 1996